Hydrogenation of acetylene–ethylene mixtures on Pd catalysts: computational study on the surface mechanism and on the influence of the carbonaceous deposits

Dario Duca *, Giampaolo Barone and Zsuzsanna Varga

Dipartimento di Scienze Farmaceutiche, Università di Salerno, Via Ponte don Melillo, I-84084 Fisciano, Salerno, Italy
E-mail: dduca@unisa.it

Received 15 August 2000; accepted 5 December 2000

A time-dependent Monte Carlo algorithm was employed to study the effects of carbonaceous surface species on the hydrogenation mechanism of acetylene–ethylene mixtures on a Pd catalyst. Simulations of tail-end and front-end mixture hydrogenation were performed employing the same set of predetermined event probabilities. The involvement of the steric hindrance of the surface species was essential to simulate the experimental data. The catalyst activity and selectivity were promoted or inhibited by different concentrations of surface polymeric species formed along with the hydrocarbon hydrogenation. Tools to get a new interpretation of the catalytic reaction mechanism and an innovative basis to perform catalyst design were suggested by the approach illustrated.

KEY WORDS: acetylene–ethylene hydrogenation mechanism; carbon deposits; time-dependent Monte Carlo

1. Introduction

Acetylene–ethylene hydrogenation on metal catalysts was thoroughly investigated [1] both as model and industrial reaction. Some main points that every mechanistic hypothesis on the reaction must account for, resulted fixed by these studies:

- The macroscopic reaction, usually represented [2] by scheme 1, must be determined by simple microscopic surface events [1,3,4] not depending on the composition of the reaction mixture.

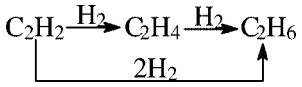

Scheme 1

- The amounts of acetylene and ethylene adsorbed on metal surfaces are comparable when the adsorption of the hydrocarbons occurs separately. The ethylene adsorption slows dramatically down [5] when ethylene is adsorbed competitively with acetylene.
- The fast deactivation of the catalyst, occurring along with the ethylene hydrogenation, is inhibited by the presence of acetylene in the reaction mixture. Moreover, a previously performed acetylene hydrogenation on a catalyst can increase the ethylene hydrogenation rate on the same catalysts [4]. However, the introduction of acetylene in a H_2/C_2H_4 reaction mixture cannot reactivate a catalyst already deactivated by the ethylene hydrogenation.
- Parallel reactions occur on the surface with the hydrogenation of unsaturated hydrocarbons. These parallel processes produce polymer and carbonaceous species [6], which mostly remain adsorbed on the surface.
- Although alkenes are almost not hydrogenated in presence of just traces of alkynes or alkadienes, their hydrogenation, on the same metal surfaces, shows a reaction rate of the same order of magnitude of that of the alkynes or alkadienes both in heterogeneous bi- (gas–solid) [3,4] and tri- (gas–liquid–solid) phase systems [7–9].
- The mutual interactions of the surface species, reacting, coating, ageing, considerably influence, by promoting and/or poisoning, the activity and selectivity of the catalyst [1,3,4,7–12].

The last point is even supported by experimental findings showing that the acetylene hydrogenation rate increases with the increasing formation, among the reaction products, of C_4 species [13]. These can be considered as species monitoring the composition of the surface deposits and since the amount of them is mainly determined by their intra-molecular steric hindrance and not by their energetics, it can be inferred that the steric hindrance of the surface molecules could influence the composition of the reaction products.

A deterministic algorithm modelling the surface mechanism of the title reaction [3,4] was used to study the dynamic modifications of the surface sites of the catalysts employed in the unsaturated hydrocarbon hydrogenation. This approach, surface site evolution model (SSEM), showed that at least four different sites should be present on the surface.

* To whom correspondence should be addressed.

1011-372X/01/0300-0017$19.50/0

The originally proposed scheme [3,4], which was stressing the function of three of the sites above, is in the present paper modified as in scheme 2.

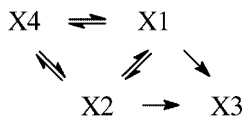

Scheme 2

In this scheme, X1 sites are the starting sites, which can interact with every species involved in the surface reaction. X1 sites should be transformed during the reaction, reversibly to X4 and X2 and irreversibly to X3 sites.

Actually, X2 sites are accessible to the less hindering hydrocarbon species, e.g., in the mixture acetylene–ethylene just to acetylene, whereas X4 sites can interact only with hydrogen and X3, being irreversibly coated by carbonaceous deposits, with no species.

Studies, performed by home-made time-dependent Monte Carlo [14,15] (tdMC) algorithms, recently confirmed the findings above and explained [1], bringing new microscopic details [1,16,17], the genesis of the different reactivity found on the distinct sites. A peculiar result of the tdMC applications on the catalysed hydrocarbon hydrogenation was that hindering carbonaceous surface deposits although subtracting catalyst sites could increase the catalytic hydrogenation rate [18]. Interestingly, these findings reproduced experimental details[19] reported by Jackson et al.

The role of the carbonaceous deposits on the surface reactivity is still undetermined [6]. Particularly, for the catalytic hydrocarbon hydrogenation, it has been hypothesised that carbonaceous surface deposits, by uniformly coating the metal surface, hence changing the electronic properties of the surface, actually behave as the effective catalytic centres [11]. A different hypothesis on the influence of the carbonaceous formation involves the partial coating of the surface by the deposits, which determine surface decorations. These, by geometrical effects probably related to the steric hindrance of the reacting species [15], should drive the metal surface reactivity [1,3,4,10]. However, these hypotheses are not mutually in conflict and the superimposition of the two mechanisms could also occur [3,4].

In this paper we show that the geometrical effects determined by the steric hindrance of the surface species could have, at least in the hydrocarbon hydrogenation, a fundamental role in the catalytic mechanism of the surface reaction.

2. Information on the approach and model

This work presents a comparison between experimental [3] and tdMC activity and selectivity data of acetylene–ethylene mixture hydrogenation on a progressively aged Pd catalyst, occurring in a continuous-flow fixed-bed reactor. Both front-end [3,4] (acetylene traces in ethylene-rich feedstock containing hydrogen amount comparable with that of ethylene) and tail-end [3,4] (acetylene traces in ethylene-rich feedstock containing hydrogen amount comparable with that of acetylene) mixtures were examined. Turnover frequency for the acetylene, $\mathrm{TOF}_{\mathrm{C_2H_4}}$, and ethylene, $\mathrm{TOF}_{\mathrm{C_2H_6}}$, conversion and the selectivity to ethane, S_{E} [20], were, respectively, employed to test the experimental activity and selectivity of the catalyst [3].

S_{E} is the percent ratio of the number of formed ethane molecules per number of converted acetylene molecules. In the simulations, the catalyst activity was monitored by the statistical equivalent [18] of $\mathrm{TOF}_{\mathrm{C_2H_4}}$ whereas the simulated S_{E} as

$$S_{\mathrm{E}} = \frac{\mathrm{TOF}_{\mathrm{C_2H_6}}}{\mathrm{TOF}_{\mathrm{C_2H_4}}} \times 100,$$

where $\mathrm{TOF}_{\mathrm{C_2H_6}}$ is the statistical equivalent of the turnover frequency for the ethylene conversion. Note that the same symbols ($\mathrm{TOF}_{\mathrm{C_2H_4}}$, $\mathrm{TOF}_{\mathrm{C_2H_6}}$ and S_{E}) were employed for experimental and simulated data.

The Horiuti–Polanyi, HP, model employed in the work is detailed by the following steps:

$$\mathrm{H_2} + 2* \rightleftharpoons 2\mathrm{H}(*)$$

$$\mathrm{C_2H_2} + 2* \rightleftharpoons \mathrm{C_2H_2}(*)_2$$

$$\mathrm{C_2H_4} + 2* \rightleftharpoons \mathrm{C_2H_4}(*)_2$$

$$\mathrm{C_2H_6} + 2* \rightleftharpoons \mathrm{C_2H_6}(*)_2$$

$$\mathrm{C_2H_2}(*)_2 + \mathrm{H}(*) \rightleftharpoons \mathrm{C_2H_3}(*)_2 + *$$

$$\mathrm{C_2H_4}(*)_2 + \mathrm{H}(*) \rightleftharpoons \mathrm{C_2H_5}(*)_2 + *$$

$$\mathrm{C_2H_3}(*)_2 + \mathrm{H}(*) \rightarrow \mathrm{C_2H_4}(*)_2 + *$$

$$\mathrm{C_2H_5}(*)_2 + \mathrm{H}(*) \rightarrow \mathrm{C_2H_6}(*)_2 + *$$

$$\mathrm{C}_x\mathrm{H}_y(*)_m + \mathrm{C}_w\mathrm{H}_z(*)_n \rightarrow \mathrm{C}_{(x+w)}\mathrm{H}_{(y+z)}(*)_{(m+n)}$$

$*$ and $(*)$ are empty and occupied surface sites whereas $\mathrm{X}(*)_n$ are X species adsorbed on n adjacent catalytic sites. The last step represents the formation of the carbonaceous deposits.

Adsorption, desorption, diffusion and reacting events were considered and periodic boundary conditions were introduced on the {100} and {111} simulated surfaces [1]. Square matrices, usually characterised by 100×100 elements (sites), were employed to simulate the surfaces above [1]. Since continuous-flow reactor processes were simulated, the individuation of the number of molecules present in the vapour phase was not essential [1]. Moreover, the different metal planes considered did not affect the simulation results.

Further, mathematical and physical details on the HP model, on the mimicked surfaces, on the event probabilities, on the random number generator, on the platforms, on the computing time and, generally, on the tdMC algorithm employed in the simulations of this work, can be found in [1].

Here, it is to be underlined that the present model emphasises the function of the steric hindrance of the species (reagents, products and deposits) involved in the surface reaction [15] and shows that the same steric hindrance becomes fundamental in explaining the findings pointed in the previous section.

Here, the steric hindrance of the surface species is defined by the interaction probability, Π_I, model. The values of Π_I for the surface reagents were determined, as reported [17], by a Monte Carlo approach using experimental results published by Yasumori et al. [21]. Conversely, for the carbonaceous deposits, here also called *alter*, variable values of Π_I and of the percentage of the surface covered by *alter*, alter%, were considered.

We suggest the term *alter* because, as will be shown, the same carbonaceous deposits can have both increasing, promoter, or decreasing, poison, outcomes on the activity and selectivity of a given surface process. Hence, *a priori*, it can be just inferred that these deposits have *alter*ation effects on the same process.

3. Results and discussion

Taking into account the experimental conditions to be reproduced, the event probabilities employed in the simulations were calculated as reported in [1] by the collision or the stationary state theory. Whenever possible, the parameters involved in the calculation of the event probabilities, functional expressions of the partition function and activation energies of the events, were determined by quantum mechanical computations [1,18].

Front- and tail-end mixture hydrogenation on the same supported, 0.05% Pd/pumice, catalyst having a metal dispersion, D_X, equal to 0.65 [3] were mimicked. The simulated total pressure of front- and tail-end feedstock was 1 atm, the exact composition of the mixtures being those reported in [3]. The simulated temperatures were 303 and 323 K for the front- and tail-end mixture, respectively. The activity and selectivity contour maps (see below) reported in this paper were obtained considering simulated values of these parameters determined at chemical regime [1,18,22] and steady state conditions [1].

Experimentally [3], the space velocities were set to have comparable acetylene rate conversion in the two mixtures. This allowed us to compare the simulated catalyst surface changes caused by the front- and tail-end hydrogenation. Simulations were performed mimicking given percentages of inhibited sites, alter% values, by carbonaceous species having different Π_I.

Figures 1 and 2 show contour maps, depending on alter% and Π_I, of activity (figures 1(a) and 2(a)) and selectivity (figures 1(b) and 2(b)) of front-end (figure 1 (a) and (b)) and tail-end mixtures (figure 2 (a) and (b)). Fifty simulations, considering regularly distributed values of alter% (0–50%) and Π_I (0–1), followed by an interpolation procedure, were employed to draw every pair of pictures. In the pictures, activity and selectivity are reported as relative values, TOF-r and S_E-r parameters. The experimental values of TOF-r and S_E-r were obtained by considering the ratios between the values of $TOF_{C_2H_4}$ or S_E at a given reaction time with respect to their values at the starting reaction time [3]. The simulated TOF-r and S_E-r values were achieved normalizing the $TOF_{C_2H_4}$ and S_E values, obtained by given pairs of alter% and Π_I, to the values of the same

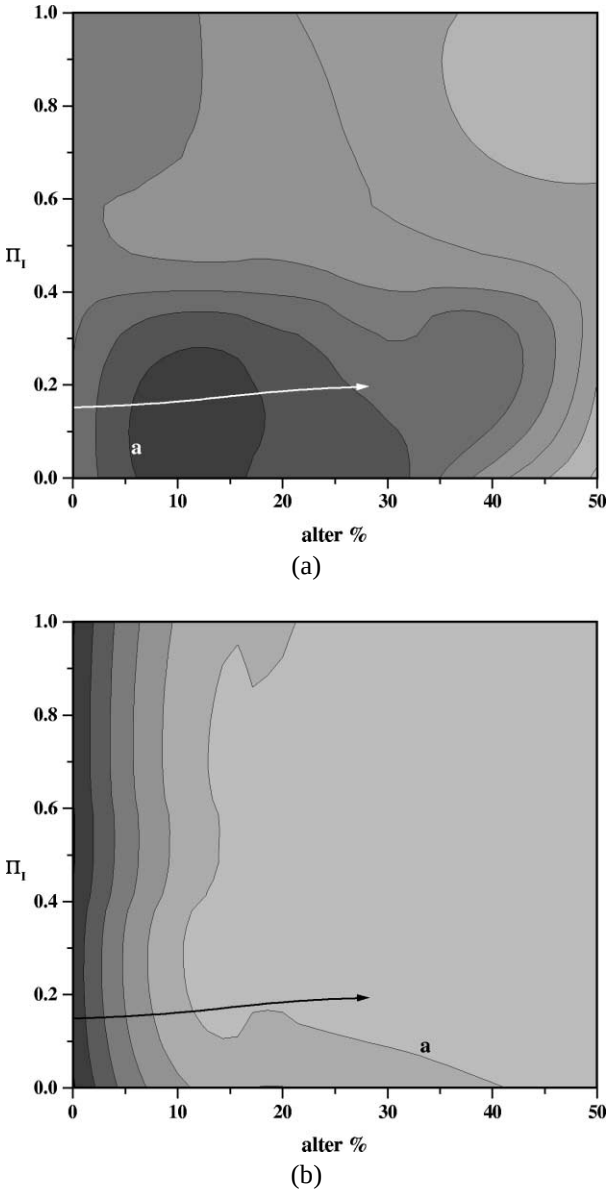

Figure 1. (a) C_2H_2–C_2H_4 front-end mixture hydrogenation on Pd catalyst: simulated TOF-r contour plot. TOF-r values increase with the grey tones. Darkest grey region represents TOF-r values ranging between 1.80 and 1.58. Contour line **a** individuates values of TOF-r equal to 1.58. Sequential lines show increasing/decreasing values of TOF-r by 0.22. The arrowed line shows a possible surface transformation path occurring along with the front-end hydrogenation. (b) Simulated S_E-r contour plot. S_E-r values increase with the grey tones. Lightest grey region represents S_E-r values ranging between 0.00 and 0.10. Contour line **a** individuates values of S_E-r equal to 0.10. Sequential lines show increasing/decreasing values of S_E-r by 0.10. The arrowed line shows the surface transformation path of (a).

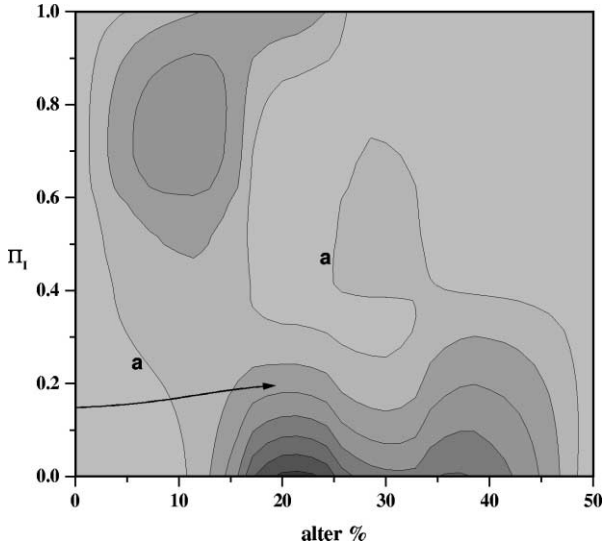

(a)

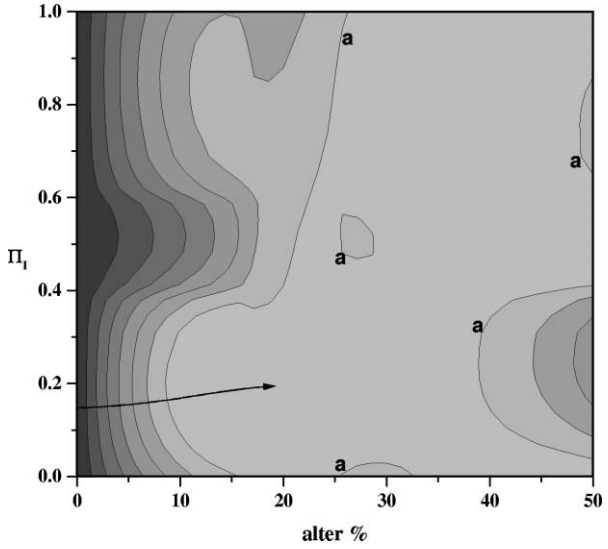

(b)

Figure 2. (a) C_2H_2–C_2H_4 tail-end mixture hydrogenation on Pd catalyst: simulated TOF-r contour plot. TOF-r values increase with the grey tones. Lightest grey region represents TOF-r values ranging between 0.00 and 0.28. Contour lines **a** individuate values of TOF-r equal to 0.28. Sequential lines show increasing/decreasing values of TOF-r by 0.28. The arrowed line shows a possible surface transformation path occurring along with the tail-end hydrogenation. (b) Simulated S_E-r contour plot. S_E-r values increase with the grey tones. Lightest grey region represents S_E-r values ranging between 0.00 and 0.13. Contour lines **a** individuate values of S_E-r equal to 0.13. Sequential lines show increasing/decreasing values of S_E-r by 0.13. The arrowed line shows the surface transformation path of (a).

parameters when alter% and Π_I were 0 and 1, respectively. Considering that the last conditions are those of the fresh catalyst, corresponding to the catalyst conditions at the starting reaction time, simulated TOF-r and S_E-r values actually reproduce the experimental ones. Since the relative values of activity and selectivity of only one catalyst were considered in this work, the simulated system was simplified considering non-influent the geometrical and electronic effects of the different kinds of catalytic sites. Hence available surface energy, ASE, distributions [1,18], which could also account of parasitic effects (e.g., bi-functionality and spillover) [23], and the metal dispersion [1,18] were not introduced in the simulations reported in this paper.

Note that the symbols TOF-r and S_E-r are used for both experimental and simulated systems.

Formation of carbonaceous deposits is a slower [6] process than the parallel surface hydrogenation. Therefore, figures 1 and 2 summarise possible evolution paths of activity and selectivity with the ageing of the catalyst surface when front- and tail-end mixtures hydrogenation is performed. However, any information on the evolution time is not achievable from the same figures.

Figures 1(a) and 2(a) clearly show that, due to geometrical effects, an increasing TOF-r can occur also subtracting active sites to the catalyst. This finding is not surprising since the surface hydrogen amount is little influenced by the presence of other surface species [1] while hydrogenation of acetylene in acetylene–ethylene mixtures is strongly influenced by the relative amount of the hydrocarbon species, reagents and deposits, on the catalyst. In fact, ethylene has higher steric hindrance than acetylene, e.g., Π_I values at 298 K are [1,17,18] 0.05 and 0.25, respectively, and due to their steric interactions with the surface deposits it is possible to observe, by analysing [1,15] the mimicked surface, that increasing the carbonaceous formation, the relative amount of acetylene increases with respect to that of ethylene, which results also surrounded by the same acetylene molecules. However, we did not observe a simple correlation between the increasing of the acetylene/ethylene ratio and the activity/selectivity pattern of the studied catalytic reactions.

Experimental hydrogenation of front-end mixture [3] showed:

(i) In the first 25 min TOF-r increased to 1.2, then slowly decreased up to reach, after 450 min, the value 1.0. In this period, S_E-r decreased about five times.

(ii) SSEM shows that corresponding to the maximum of TOF-r, the percentage of the inhibited sites, X3, becomes almost constant and about equal to 70%. At the same time, X1 and X2 sites slowed down to 0% and increased to 30%, respectively.

Conversely, experimental hydrogenation of tail-end mixture [3] showed:

(i) In the first 40 min TOF-r increased to 1.1 and then remained constant. Along the time of the experiment, 450 min, S_E was almost constant.

(ii) SSEM shows that corresponding to the maximum of TOF-r, the percentage of X3, X2 and X1 becomes almost constant and about equal to 85, 15 and 0%.

tdMC simulations were able to reproduce experimental selectivity and activity results, collected in the first 30–40 min [3] of catalyst use, by introducing surface coverage of carbonaceous deposit having $\Pi_I = 0.15$, of 15 and 27.5%

for the tail- and front-end [1], respectively. Considering the collecting time range, it can be hypothesised that the coverage percentages above are coincident with those present when the equilibrium conditions among the different surface sites are reached in the ageing experiment of this work, for tail- and front-end, respectively. Moreover, it is reliable to state that the starting Π_I of the carbonaceous deposits has a value between that of acetylene and ethylene [1], most likely 0.15. Since the presence of these deposits selectively increases the acetylene surface population [1], the Π_I values of the same carbonaceous species should increase in the time up to that of the acetylene. We excluded higher Π_I because of the relatively low temperature of the simulated ageing experiments, see above and [3], which likely rules out the involvement of surface dehydrogenation phenomena.

The two pairs of figures 1 (a, b) and 2 (a, b) show arrowed lines that are identical for any pair of figure. These lines represent possible evolution paths of carbonaceous formation on the catalyst surface. In fact, they start from Π_I equal to 0.15 and, moving toward the Π_I value of the acetylene, reach the alter% values previously obtained [1] for the front- and tail-end mixtures. The two paths of carbonaceous deposit formation reported in figures 1 (a, b) and 2 (a, b) properly represent the experimental TOF-r and S_E-r. However, the same paths are not able to give any information on the time in which the changes occur on the surface.

Better agreement between the experimental and simulated results of TOF-r and S_E-r is achieved if the starting point, i.e., the time of the first experimental measurement, of the surface evolution path is set at alter% values of 1.5 and 10 for the front- and tail-end mixture, respectively. In this case, a preliminary deposition of *alter* species, more significant in the hydrogenation of the tail-end mixture, should occur very rapidly on the surface, few seconds in the experimental condition considered here [3]. Slower deposition processes of other carbonaceous species should follow this occurrence.

The analysis above illustrates a new hydrogenation surface mechanism which occurs by events arising on non-coated metallic sites and controlled by the steric hindrance of the surface reagents and of the *alter* species, which are formed by processes taking place in parallel to the hydrogenation.

An apparent disagreement between SSEM [3] and tdMC results concerns the absolute and the relative values of the equilibrium percentage of hindered sites on the surface. In fact, SSEM percent values are 70 and 85%, and tdMC 27.5 and 15% for front- and tail-end mixtures, respectively. However, carbonaceous species having Π_I equal to 0 and coating the surface by alter% equal to 15, actually hinders a 75% of surface sites. Consequently, the difference between the SSEM and tdMC values of the percentage of hindered surface sites is not critical. The same is true for the inversion of the values we found between front- and tail-end mixtures. Indeed, it has been found that in the front-end mixture hydrogenation the surface amount of $C_2H_4 + C_2H_5$ species is larger than in the tail-end mixture hydrogenation and that moreover, the other surface molecules surrounded these species, which because of this were hydrogenated [1] with difficulty. So, if the number of the sites coated by carbonaceous and ethylene species [1] at the equilibrium are added up, we found that the percentage of surface occupied is 50 and 63% for the front- and the tail-end, respectively. Of course, as before, the percentages of the inhibited sites have to be increased due to the Π_I values of the considered surface species.

Table 1
Surface population found[a] by tdMC simulations on a Pd {100} plane at constant atmospheric pressure and different temperature and vapour phase composition.

Vapour phase	Surface species C_2H_2|C_2H_4[c]			
C_2H_2/C_2H_4[b]	$T = 270$ K	$T = 290$ K	$T = 310$ K	$T = 330$ K
1.00/0.00	0.796|0.000	0.796|0.000	0.799|0.000	0.804|0.000
0.75/0.25	0.694|0.095	0.704|0.088	0.773|0.019	0.791|0.005
0.50/0.50	0.575|0.223	0.682|0.103	0.767|0.013	0.782|0.003
0.25/0.75	0.388|0.387	0.514|0.251	0.707|0.038	0.753|0.007
0.00/1.00	0.000|0.674	0.000|0.605	0.000|0.558	0.000|0.512

[a] Activation energy of the adsorption, desorption and diffusion events of the involved species are reported in [1]. The description of the algorithms employed to calculate the event probabilities are also reported in the above paper. However, due to the characteristics of the events mimicked in this work, it was possible, by minor changes in the program [24], to simulate processes occurring in 0.1–0.2 s.

[b] Vapour phase is formed by just acetylene and ethylene. In $x.xx/y.yy$ ratio, $x.xx$ and $y.yy$ values are the molar ratio of the species C_2H_2 and C_2H_4.

[c] $x.xxx$ and $y.yyy$, in $x.xxx|y.yyy$, are the surface molar ratio values at the given temperatures, of C_2H_2, and C_2H_4, respectively. The residual are unoccupied sites. The molar ratios are obtained by surface population values averaged at steady state conditions.

The X1 site evolution of SSEM is well in agreement with the surface population changes found by the tdMC simulations. Whilst, considering the Π_I of the acetylene molecules, also the equilibrium values of the X2 site percentage achieved by SSEM, for both the feed-stocks considered, are pretty in accord with the percentage of the sites available for the same acetylene. Sites accessible just to hydrogen species, i.e., X4 sites, were not explicitly considered in the original SSEM approach [3,4] since we considered these species as homogeneously distributed on the surface. However, regarding the surface hydrogen atoms like point species [1], we can identify the X4 sites with those uncovered and still obstructed by hindering surface species. Therefore, it is clear that, although less detailed, SSEM gives information coherent to that achieved by the tdMC simulations.

tdMC algorithm, employed to simulate adsorption–desorption processes on a {100} Pd plane of mixtures containing only ethylene and acetylene at a total atmospheric pressure, in a wide range of temperatures showed that, irrespective of the initial vapour ratio, acetylene is always the largest component of the surface population. Table 1 summarises the results of the adsorption–desorption simulations above. It shows that regardless of the equilibrium temperature the amount of acetylene on the surface is almost

constant when pure acetylene vapour phase is considered. Moreover, table 1 also shows that irrespective of the vapour acetylene/ethylene molar ratio, acetylene always covers a larger fraction of surface sites. In spite of this, at given temperatures, the time necessary to reach the equilibrium population on the surface was comparable for the adsorption from the gas phase of pure acetylene or ethylene. Remarkably, simulated tdMC hydrogenation rate of pure ethylene [1,13,18] showed, as experimentally found [3,4,8], the same order of magnitude of that of acetylene for comparable hydrocarbon/hydrogen ratio. Having considered similar activation energy involved [1] in the hydrogenation events of alkynes and alkenes, the findings above are in agreement with the results of the surface population analysis performed during the adsorption–desorption simulated experiments.

In fact, the low amount of the surface hydrogen, producing the first reaction order with respect to the same hydrogen [1,15,18], results almost unchanged in the two considered systems, acetylene hydrogenation and ethylene hydrogenation, whereas the surface percent changes on the very large amount of surface hydrocarbon (acetylene or ethylene), which origins its typical zero reaction order, does not affect the hydrogenation rates.

In conclusion, our simple model based on the sequential occurrence of simple events, captures the main characteristics involved in the hydrocarbon hydrogenation and pointed in section 1 of this paper.

The resulting energetics of the hydrocarbon hydrogenation on a metal catalyst have to be strongly affected by the surface decoration, shaped by the surface species, which should drive the adsorption–desorption and diffusion processes and the relative hydrogenation and polymerisation rates. With this we do not exclude that the surface species could influence the electronic properties of the surface [1], which certainly are also conditioned by the shape and the size of the metal particles. Hence, we do not exclude other possible factors affecting [1,18] the reactivity of the catalyst. However, we think that when the same catalyst is used for hydrocarbon hydrogenation in different experimental conditions, the decisive features must be looked for on the surface decoration effects. In our opinion, these surface formations influence also the relative amounts of the polymerisation products, which therefore could grow, independently by their thermodynamic stability, just conditioned by their intra-molecular steric hindrance, see section 1 of this paper.

Finally, it has to be pointed out that the activity and selectivity contour maps, never presented before now, can be built by mimicking a given catalytic process depending on two or more parameters and then can be employed to design *ad hoc* metal surfaces to be used in specific working conditions of the same catalytic system.

4. Conclusion

In this work, employing a time-dependent Monte Carlo algorithm, we tried to enclose the available element of experience on the title reaction in a coherent system of general ideas. The results of the approach are in agreement with the main experimental findings. They reproduce pieces of evidence and justify apparent discrepancies among them.

The different steric hindrance is presented as a crucial parameter in characterising the activity–selectivity pattern of a catalyst. The current idea on the role of promoter and poison species is criticized and it is shown that, at least for the acetylene–ethylene mixture hydrogenation, the same surface species may have positive, negative or also null effect on the surface reactivity. Particularly, it is underlined that the decreasing of the number of the surface sites does not always determine the decreasing of the surface activity and conversely, it can produce opposite effects.

Selectivity and activity surfaces can be built up by using tdMC simulation data. The analysis of these surfaces suggests that the same ones can be used for getting new insights on the studied reaction and for designing new catalysts with specific properties.

References

[1] D. Duca, G. La Manna, Zs. Varga and T. Vidöczy, Theor. Chem. Acc. 104 (2000) 302.
[2] R. Pestman, A.J. den Hartog and V. Ponec, Catal. Lett. 4 (1990) 287.
[3] D. Duca, F. Frusteri, A. Parmaliana and G. Deganello, Appl. Catal. A 46 (1996) 269.
[4] D. Duca, F. Arena, A. Parmaliana and G. Deganello, Appl. Catal. A 172 (1998) 207.
[5] Z. Hlavathy, P. Tétényi and Z. Paál, J. Chem. Soc. Faraday Trans. 88 (1992) 2059.
[6] G. Bond, Appl. Catal. A 3 (1997) 149.
[7] G. Deganello, D. Duca, A. Martorana, G. Fagherazzi and A. Benedetti, J. Catal. 150 (1994) 127.
[8] D. Duca, L.F. Liotta and G. Deganello, J. Catal. 54 (1995) 69.
[9] D. Duca, G. La Manna and G. Deganello, Catal. Lett. 52 (1998) 73.
[10] A. Borodzinski and A. Golebiowski, Langmuir 13 (1997) 887.
[11] S.J. Thomson and G. Webb, J. Chem. Soc. Chem. Commun. (1976) 526.
[12] W.T. McGown, C. Kemball, D.A. Whan and M.S. Scurrell, J. Chem. Soc. Faraday Trans. 73 (1977) 632;
A.S. Al-Ammar and G. Webb, J. Chem. Soc. (Faraday Trans.) 74 (1978) 195, 657; 75 (1979) 1990;
J. Margitfalvi, L. Guczi and A.H. Weiss, J. Catal. 72 (1981) 185;
G.F. Berndt, S.J. Thomson and G. Webb, J. Chem. Soc. Faraday Trans. 79 (1983) 195;
J.H. Moses, A.H. Weiss, K. Matusek and L. Guczi, J. Catal. 86 (1984) 88;
J. Houzvicka, R. Pestman and V. Ponec, Catal. Lett. 30 (1984) 289;
S. Asplund, C. Fornell, A. Holmgren and S. Irandoust, Catal. Today 24 (1995) 181;
S. Asplund, J. Catal. 158 (1996) 267.
[13] D. Duca and T. Vidöczy, in: *Proc. 14th Int. Conf. Chem. Reactor*, Tomsk, 1998 (Boreskov Institute of Catalysis, Novosibirsk, 1998) p. 21.
[14] B.J. Garrison, P.B.S. Kodali and D. Srivastava, Chem. Rev. 96 (1996) 1327.
[15] D. Duca, L. Botár and T. Vidóczy, J. Catal. 162 (1996) 260;
D. Duca, P. Baranyai and T. Vidóczy, J. Comput. Chem. 19 (1998) 396.
[16] G. La Manna, G. Barone, Zs. Varga and D. Duca, Int. J. Quantum Chem., in press.
[17] D. Duca, G. Barone, Zs. Varga and G. La Manna, J. Mol. Struct. (Theochem), submitted.

[18] D. Duca, G. La Manna and M.R. Russo, Phys. Chem. Chem. Phys. 1 (1999) 1375.
[19] S.D. Jackson, G.D. McLellan, G. Webb, L. Conyers, M.B.T. Keegan, S. Mather, S. Simpson, P.B. Wells, D.A. Whan and R. Whyman, J. Catal. 162 (1996) 10.
[20] G.C. Battiston, L. Dalloro and G.R. Tauszik, Appl. Catal. 2 (1982) 1.
[21] I. Yasumori, H. Shinohara and Y. Inoue, in: *Proc. 5th Int. Congr. on Catalysis*, Palm Beach, 1972 (North-Holland, Amsterdam, 1973) p. 53/1.
[22] J.R. Madon and M. Boudart, Ind. Eng. Chem. Fundam. 21 (1982) 438.
[23] M. Boudart and G.D. Mariadassou, *Kinetics of Heterogeneous Catalytic Reactions* (Princeton Univ. Press, Princeton, NJ, 1984).
[24] D. Duca, to be published.